Indian Journal of Pure & Applied Physics
Vol. 63, June 2025, pp. 460-466
DOI: 10.56042/ijpap.v63i6.8511

Reliable EAR Method to Increase the Performance of a Solar PV Array connected in TCT fashion even in Partial Shading Condition

Papul Changmai[1*], Jesif Ahmed[2], Sanjib Kalita[3], Deba Kumar Mahanta[4], Himanshu Sekhar Sahu[5] & Abhijit Bora[6]

[1,2]Department of EEE, Assam Don Bosco University, Guwahati 781 017, India

[3]Department of ECE, NIT Arunachal Pradesh, Arunachal Pradesh 791 123, India

[4]Department of EE, Assam Engineering College, Guwahati 781 013, India

[5]Department of EE, Shiv Nadar University, Greater Noida 201 314, India

[6]Department of CA, ADBU 781 017, India

Received: 3 February 2024; accepted: 9 May 2025

In partial shading condition (PSC), the solar photo-voltaic (PV) array's efficiency is significantly reduced. Although using a bypass diode increases the efficiency of a PV array that is connected in series, it also causes problems with multiple peaks (local and global peaks). Total-Cross-Tied (TCT) connections are suggested in the literature as a solution to these problems. Despite having superior performance when compared to other configurations like SP, bridge links, honeycomb, etc., the TCT-connected PV array does not provide satisfactory results for all types of shading patterns. This work proposes a robust algorithm to address these problems, allowing PV installers to achieve high efficiency under any type of shading pattern. The electrical array reconfiguration (EAR) technique is used in the proposed algorithm. The results of laboratory-scale experiments and MATLAB simulations used to verify the proposed model demonstrate extremely close coordination.

Keywords: Total-Cross-Tied connection, Solar photovoltaic array, Partial shading, Irradiance

1 Introduction

As the cost of solar photovoltaic (PV) systems decreases day by day[1], the PV market is spreading across the globe at a very fast rate. As per the International Energy Agency (IEA), China's PV power capacity had reached 253 GW by 2020, or roughly 11.5 % of the country's total generating capacity. This made up one-third of the 760.4 GW installed solar capacity worldwide[2]. Improvement of the photovoltaic system's efficiency of power generation has emerged as a major research concern, which is constrained by the PV array's installation space and panel cost. The basic energy conversion component of solar power generation is the PV cell. The incident photons from the sun are used to produce electricity. In the case of several models that have been developed recently, it is possible to comprehend the performance of a PV system under various climatic conditions[3]. The PV module is made up of several cells connected in series to produce medium voltage levels, whereas a PV array is made up of several PV modules combined in various series and parallel configurations to produce greater voltage and current levels[4]. The shape of a partial shadow and the design of a PV array are the two primary factors affecting the output power generated by a PV system. Series-Parallel (SP), Triple-Tied (TT), Total-Cross-Tied (TCT), Honey-Comb (HC), Bridged-Link (BL), and other derivative hybrid forms[4] can all be used to connect a PV array.

Although the PV market has a huge potential, it has some demerits which occur as an obstacle in the growth of the market, e.g., the efficiency of PV systems degrades severely in partial shading conditions. Normally, solar modules are connected in SP connection in the existing PV plant[5]. In the SP-connected PV modules, the efficiency degradation is highest. To solve that problem, bypass diode is used, which creates multiple peaks issues (local and global peaks). In line with this, a number of connections such as bridge link (BL), Honey Comp (HC), TCT[6], etc., are introduced, out of which the TCT connection is found to be the best connection. But, from the careful observation, it is noticed that the performance of TCT-connected PV array cannot increase beyond a certain limit. Generally, if a set of adjacent modules is shaded at a time, the performance of TCT-connected array degrades drastically. So, it is of utmost importance to

*Corresponding author: (E-mail: papuljec5@gmail.com)

disperse the shadow to get high efficiency. In line with these a lot of electrical array reconfiguration (EAR) techniques, such as Sudoku, Futoshiki puzzle patterns, etc. are introduced in the literature. But most of the techniques suffer from the problem of computational complexity and convergence issues. In line with this, a robust algorithm is developed which will help to disperse the shaded area of a TCT-connected PV array.

2 Current State of Art in the PV Modeling

For straightforward analysis, many times the single-diode PV model, as shown in Fig. 1, is used. Its electrical equivalent circuit[7] is represented by a diode (D), photo current (I_{ph}), a parallel resistance (R_p) that stands in for leakage current, and a series resistance (R_S) that stands in for the internal resistance of the PV cell.

As mentioned in[8], the terminal current of the single-diode PV module can be represented by Eq 1:

$$I = I_{ph} - I_o\left[\exp\left(\frac{q}{kTA}(V + IR_S)\right) - 1\right] - \left(\frac{V + IR_S}{R_p}\right) \quad \ldots(1)$$

where I_{ph} is light-generating current, I_o is the cell saturation current or diode saturation current, T is the operating temperature of the cell in Kelvin (K), q is the electron charge (1.602×10^{-19} C), k is the Boltzmann constant (= 1.381×10^{-23} J/K) and A is the ideality constant of the diode. The solar irradiation and temperature have a significant impact on I_{ph}, which is defined as the current produced by photons as a result of incident light and is given as Eq 2:

$$I_{ph} = \frac{\left[I_{SC} + K_I\left(T - T_{ref}\right)\right]G}{G_n} \quad \ldots(2)$$

where I_{SC} is the short-circuit current of the cell at Standard Test Conditions (STC) of PV panel (i.e., at 25°C and solar irradiance of $1000 W/m^2$), T_{ref} denotes the reference temperature for the cell, K_I is the cell's short-circuit current temperature coefficient, G is the cell's solar irradiation and G_n is the nominal solar irradiation in W/m^2. The saturation current I_o varies with the cell temperature and it can be expressed as Eq 3:

$$I_o = I_{o,n}\left(\frac{T_{ref}}{T}\right)^3 \exp\left[\frac{qE_g}{Ak}\left(\frac{1}{T_{ref}} - \frac{1}{T}\right)\right] \quad \ldots(3)$$

where $I_{o,n}$ represents the nominal saturation current, E_g represents the band gap energy for the semiconductor (where E_g = 1.12 eV in case of the polycrystalline Silicon at a temperature of 25°C).

A typical PV cell has an output power of less than 2W at a voltage of 0.5 V. PV cells are coupled in a module in series as well as parallel arrangement to generate the required amount of power[7, 9]. Figure 2 depicts a PV module's electrical equivalent circuit configured in N_S series cells and N_P parallel cells.

As mentioned in[8], the terminal current equation of a PV module in series-parallel configuration is given by Eq 4:

$$I = N_P I_{Ph} - N_P I_o\left[\exp\left(\frac{q}{kTA}\left(\frac{V}{N_S} + \frac{IR_S}{N_P}\right)\right) - 1\right] - \left[\frac{\left(\frac{N_P}{N_S}\right)V + IR_S}{R_P}\right] \quad \ldots(4)$$

A particularly well-liked method for increasing output power while partially shaded is the TCT structure[8, 10]. Furthermore, the performance of a PV system is greatly influenced by the surrounding environment, including the presence of clouds, structures, and other things that create shadows on the PV system as the sun moves across. It causes PV module mismatch power loss and irradiance loss over the PV surface[11,12]. PV modules in PV arrays frequently have partial shading, and the shadow forms are typically asymmetrical. To reduce the mismatch loss in PV systems, several reconfiguration approaches, both static and dynamic, have been put forth recently[13–15].

In a static reconfiguration strategy, the generation of power is boosted before the photovoltaic system is put to use by enhancing electrical connections or

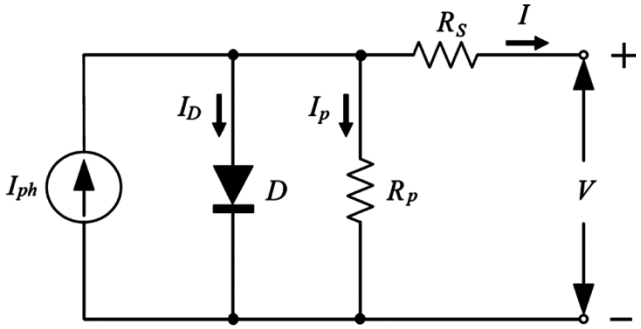

Fig. 1 — Electrical equivalent circuit of single-diode model of PV module

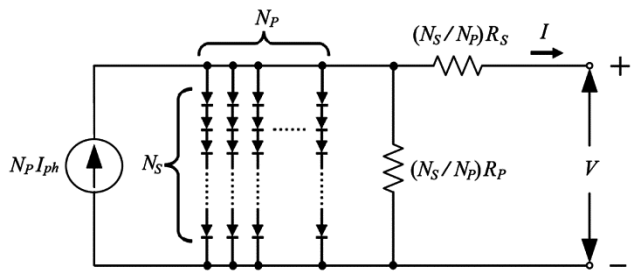

Fig. 2 — Equivalent electrical circuit of a PV module in series-parallel configuration

physical placements of PV modules. The Sudoku puzzle pattern is used to position the modules in a TCT-connected PV array such that the shadow effect is spread out throughout the entire array[13]. But when using the Sudoku approach[14], shadow dispersion is unsuccessful. A superior Sudoku reconfiguration technique is also put out in[15] in order to streamline the wire setup and improve shade coverage across the array. Additionally, the reconfiguration techniques based on the Futoshiki algorithm[16], dominant square technique[17], and LoShu methodology[18] are each put forth in turn in order to increase the power output of PV arrays. However, only square arrays may be used with any of the aforementioned techniques. Additionally, since actual shadows evolve with time, these static reconfiguration techniques cannot consistently generate maximum power.

In response to shading conditions, dynamic reconfiguration systems can modify a PV array's electrical connection. To accomplish optimal reconfiguration, a number of techniques have been put forth, such as the "irradiance equalization" approach[19], "grasshopper optimization", "particle swarm optimization with parallel computation" and "mixed integer quadratic programming"[16]. Other techniques involve operating each PV string on its own maximum power point (MPP) using a series-voltage source[20] and a two-step genetic algorithm strategy that utilizes a switching matrix to avoid partial shade[21]. The difficulties with the static and dynamic reconfiguration techniques are discussed in a comparative study[22]. Some solutions include designing the electrical connections of a PV array to toggle between TCT and SP configurations automatically under partially shaded situations[23] and using an electronic circuit based on optocoupler for each PV module, which cuts out the need for an expensive sensing and complex switching network[24]. These methods aim to minimize high costs and intricate electrical wiring in dynamic reconfiguration cases.

As is typical in other PV application domains, irregular and uneven partial shades over PV modules have been simplified in earlier studies as rectangular shapes[20]. Due to the difficulties and high cost of obtaining the precise shapes of shadows using traditional electrical sensors, the distinction between partial and complete shading of PV modules was overlooked. However, J Qi *et al*.[21] discuss the approximation error of irradiance equivalence in partially-shaded PV modules, which is motivated by effective image recognition for partial shades over PV arrays[22]. In this study, a dynamic reconfiguration strategy is modified in accordance with the irregular shadow shape, which includes data pertaining to the shaded cells number (SCN) for every PV module. Their SCN-based approach is adaptable to PV arrays with various column and row sizes and does not need enormous electrical sensors or complicated iteration computations.

Photovoltaic (PV) power has grown significantly in popularity in the field of renewable energy, especially as we move towards a low-carbon economy[23]. The rise of rooftop solar installations has been a game-changing development within the solar revolution, even if large-scale PV systems have made a considerable contribution to this increase[16]. Notably, China had a significant increase, reaching 216 GW of total installed PV capacity during the first half of 2020, with 67.07 GW coming from distributed PV systems. In the midst of this fast development, assuring the efficiency, security, and reliability of PV systems has emerged as a pressing technical imperative[24].

The effectiveness of PV arrays' power output is impacted by a variety of internal and external factors, with Array Mismatch Losses (ML) standing as a key issue caused by elements such as partial shadowing, dust, and module abnormalities[25]. Metropolitan distribution PV systems are particularly affected by the mismatch issue because of the dense population and complicated metropolitan environments. Affected modules lose power as a result, which reduces the Maximum Power Point (MPP). This is made worse by hotspots that develop from protracted partial shade, which reduces system efficiency and reliability[24]. To mitigate these issues, bypass diodes are used to redirect current around shaded or impaired modules to shield them from Mismatch Conditions (MCs)[25]. But, doing so can modify the P-V characteristic by introducing multiple peak points in it, thereby potentially complicating MPP tracking algorithms or leading to variations from the optimal MPP. Addressing these nuances is essential to maximizing the potential of PV energy and guaranteeing ongoing advancement as it continues to gain popularity.

3 Mathematical modeling of a TCT-connected PV Array

A TCT-connected PV array, along with its equivalent diagram ais shown in Fig. 3 (a) and (b), respectively. A 5×5 TCT-connected PV array is considered as shown in Fig. 4. In this figure, modules

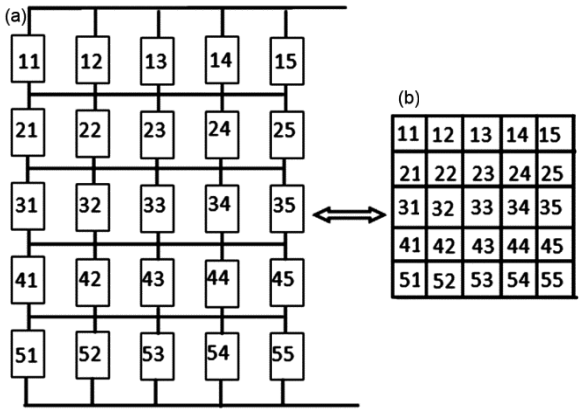

Fig. 3 — (a) TCT-connected PV array (b) Equivalent diagram of (a)

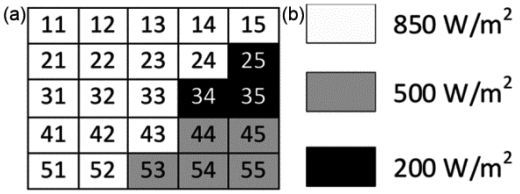

Fig. 4 — 5 × 5 TCT-connected PV array (a) shading pattern (b) index of irradiance

25, 34, 35 are shaded with 200 W/m^2, modules 44, 45, 53, 54, 55 are shaded with 500 W/m^2, and the rest of the modules are shaded with 850 W/m^2. When a module is shaded with an irradiance G_s, the generated current of that module also changes, whose value is obtained by Eq 5:

$$I = \frac{G_s}{G_{stc}} I_{mpp} \quad \ldots (5)$$

where G_{stc} and I_{mpp} are the irradiance and maximum power point (MPP) current at standard test condition (STC). At STC, the value of irradiance and temperature are considered as 1000 W/m^2 and 25 °C, respectively at 1.5 air-mass spectra. Estimating the currents generated by each module in a row, the value of the row current is obtained as given in Eq 6:

$$\begin{cases} I_1 = G_{11}I_{11} - G_{12}I_{12} + G_{13}I_{13} + G_{14}I_{14} + G_{15}I_{15} \\ I_2 = G_{21}I_{21} - G_{22}I_{22} + G_{23}I_{23} + G_{24}I_{24} + G_{25}I_{25} \\ I_3 = G_{31}I_{31} - G_{32}I_{32} + G_{33}I_{33} + G_{34}I_{34} + G_{35}I_{35} \\ I_4 = G_{41}I_{41} - G_{42}I_{42} + G_{43}I_{43} + G_{44}I_{44} + G_{45}I_{45} \\ I_5 = G_{51}I_{51} - G_{52}I_{52} + G_{53}I_{53} + G_{54}I_{54} + G_{55}I_{55} \end{cases} \quad \ldots (6)$$

In Eq 6, the value of different irradiance constants such as G_{11}, G_{25}, G_{44} etc. are obtained as given in Eq 7:

$$\begin{cases} G_{11} = \dfrac{850}{1000} \\ G_{25} = \dfrac{200}{1000} \\ G_{44} = \dfrac{500}{1000} \end{cases} \quad \ldots (7)$$

Table 1 — Power generated by the shading pattern shown in Fig. 4

Row No.	Voltage	Current	Power
1	$1\times Vmpp$	$4.25\times Impp$	$4.25\times VmppImpp$
2	$2\times Vmpp$	$3.6\times Impp$	$7.2\times VmppImpp$
3	$3\times Vmpp$	$2.95\times Impp$	$8.85\times VmppImpp$
4	$4\times Vmpp$	$3.55\times Impp$	$14.2\times VmppImpp$
5	$5\times Vmpp$	$3.2\times Impp$	$16\times VmppImpp$

Summarizing the above concept, a general expression can be written to obtained the current in the i^{th} row as Eq 8:

$$I_i = \sum_{j=1}^{n} (G_{ij} I_{ij}) \quad \ldots (8)$$

In Eq 8, I_{ij} is the MPP current at STC, which is same for all identical PV modules. Normally, in an array, all the modules are of identical in nature. $I_{ij} = I_{mpp}$. Using Eqs (7) and (8), the row currents is obtained from Eq 6, which is given in Eq 9.

$$\begin{cases} I_1 = 5 \times 0.85 I_{mpp} \\ I_2 = 4 \times 0.85 I_{mpp} + 0.2 I_{mpp} \\ I_3 = 3 \times 0.85 I_{mpp} + 2 \times 0.2 I_{mpp} \\ I_4 = 3 \times 0.85 I_{mpp} + 2 \times 0.5 I_{mpp} \\ I_5 = 2 \times 0.85 I_{mpp} + 3 \times 0.5 I_{mpp} \end{cases} \quad \ldots (9)$$

The voltage of the PV array is obtained by adding all the voltages generated by each row. After a lot of simulations and experimental results, it is observed that the partial shading has a very negligible effect on voltage variation. In the laboratory-scale experiment, a very small temperature difference is observed between the shaded modules and the unshaded modules. So, the voltage variation due to temperature constant (K_v) is also negligible. The array voltage (V_{array}) is obtained by Eq 10:

$$V_{array} = \sum_{i=1}^{n} V_{mpp_i} \quad \ldots (10)$$

where V_{mpp_i} is the MPP voltage of the i^{th} row at STC, 'n' is the total number of rows in the array. At STC, the MPP voltage is same for all the identical modules. Therefore,

$$V_{mpp_1} = V_{mpp_2} \ldots\ldots\ldots = V_{mpp_5} = V_{mpp_i} \text{ (say)} \quad \ldots (11)$$

Applying this algorithm, the power generated by each of the row is obtained as shown in Table 1.

From Table 1, it is observed that the row current changes according to the number of shaded modules

and the irradiance level in the modules. The lowest row-current will govern the whole array current. In this case, the 3^{rd} row current ($= 2.95 \times I_{mpp}$) is the lowest current, which governs the output current of the whole array. Therefore, the output power from the array is obtained as given in Eq 12:

$$P_{array} = 5\, V_{mpp} \times 2.95\, I_{mpp} = 14.75\, V_{mpp} I_{mpp} \quad \ldots (12)$$

From the careful observation, it is seen that the lowest row-current is one of the vital elements which controls the power generation from a TCT-connected PV plant. So, it is of utmost importance to enhance the value of lowest row-current. Although a number of shade dispersion algorithms, such as Sudoku, Futoshiki etc., are reported in the literature, their performances are not found suitable in many cases. After several simulations and experimental results, the below-mentioned vital points are observed:

(a) There is no improvement in row-current if the shaded modules are dispersed in the same row.

(b) Shade dispersion cannot improve the array power if the shaded modules are in the same column.

Keeping these in view, the proposed algorithm is developed to rearrange the modules of a TCT-connected PV array by changing the electrical connection. Therefore, the shading effect occurs in a different position, which strengthens the row-current. Unlike the existing algorithms, such as [16], special care is taken in the proposed algorithm to enhance the lowest value of row-current, which in turn improves the power generation from the array. Without changing the position of a PV module (say module 41 in Fig. 5 (a)), if the electrical connection of the module is shifted to position 21 as shown in Fig. 5 (a), the shading effect will be also occurring at position 21. In this figure, the electrical connection of module 44 is shifted to position 12 without changing the position of 44. Similarly, the electrical connections of the other modules are also changed, which is depicted in Fig. 5(b). The flow chart of the proposed model to determine the electrical connection of the TCT-connected PV array is shown in Fig. 6.

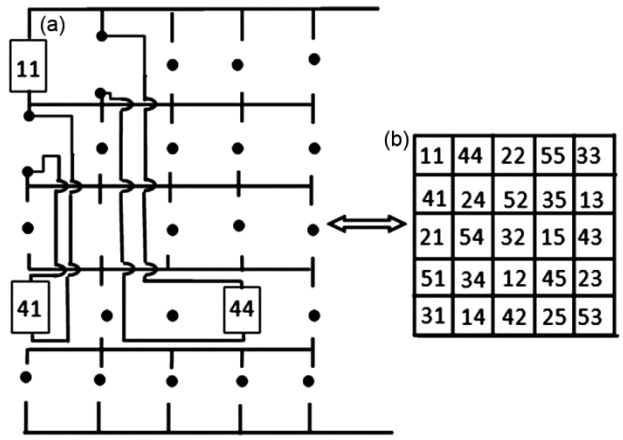

Fig. 5 — 5 × 5 TCT-connected PV array (a) Shifting of electrical connection to different position (b) Shading effect due to the change of electrical connection

To demonstrate the proposed algorithm, a 9×8 ($m \times n$) TCT-connected PV array is considered as shown in Fig. 7 (a). Here n=8, which is an even number. In Fig. 7 (b), the line AB divides the array into two equal halves. The diagonal modules 11, 22, 33... are connected sequentially in every alternate column. In the first half, the diagonal modules are connected in the first row of the array and in the second half, the same are connected in the last row of the array. After module 44, there is no more alternate column available in the array. Therefore, it is required to move back to the vacant positions and fill the gaps accordingly, starting from module 55. Once the first line of the first half and the last line of the second half is filled, it is time to fill the other positions of the array. Taking the diagonal modules as

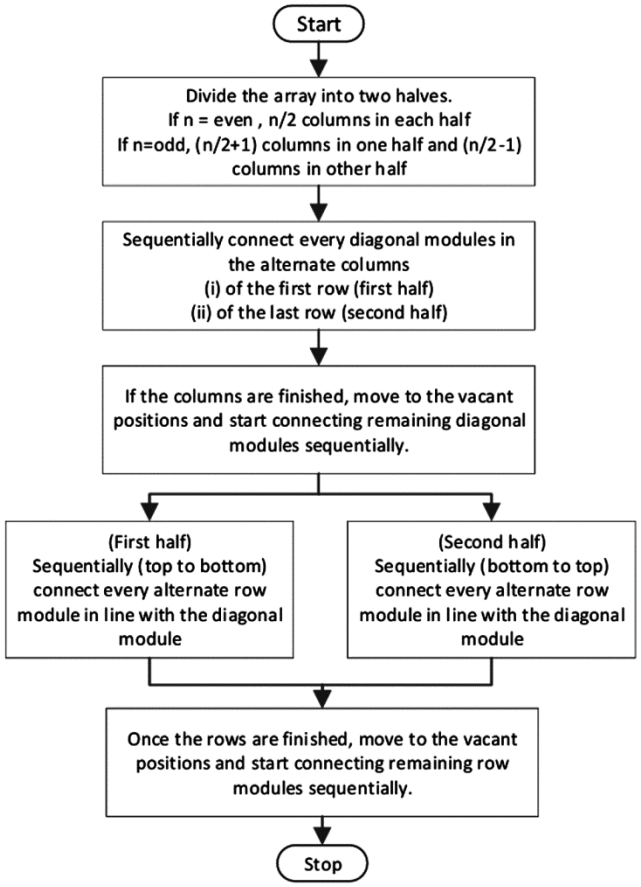

Fig. 6 — Flow Chart

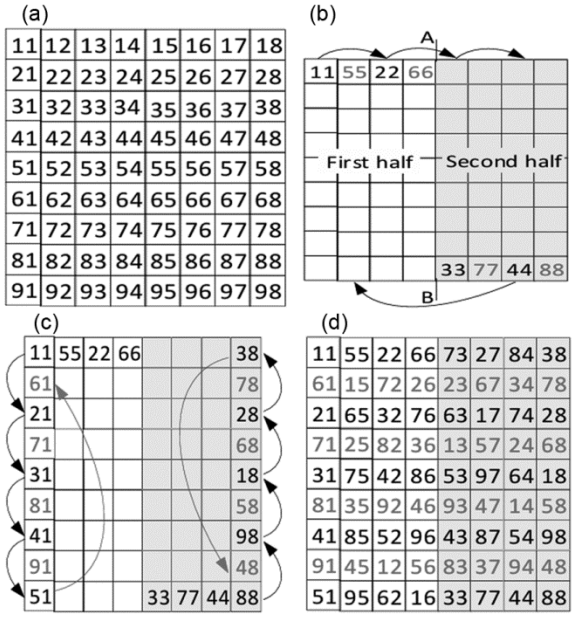

Fig. 7 — 9 × 8 TCT-connected PV array (a) equivalent diagram, (b) electrical connections of diagonal modules, (c) methodology to connect modules in every column, and (d) reconfigured 9 × 8 TCT-connected PV array

row modules are connected following exactly the same procedure which is followed for diagonal modules. For example, in the first half, taking the diagonal module 11 as reference, the other row modules such as 21, 31, 41, 51 are connected in every alternate row (downward). After module 51, it is required to move back to the vacant positions in that column and follow the same procedure as shown in Fig. 7 (c). In the second half, taking the diagonal module 88 as reference, the other row modules such as 98, 18, 28,38 are connected in every alternate row (upward). After module 38, it is required to move back to the vacant positions in that column and follow the same procedure as shown in Fig. 7 (c). Similarly, the other columns are also connected following exactly the same procedure as shown in Fig. 7 (d).

For the validation of the proposed model in 9×8 TCT-connected PV array, a partial shading condition (PSC) is considered, which is shown in Fig. 8 (a) (i).

In Fig. 8(a)(i), the modules 71-74, 81-84 and 91-94 are shaded with 0 W/m^2 irradiance, and the rest of the

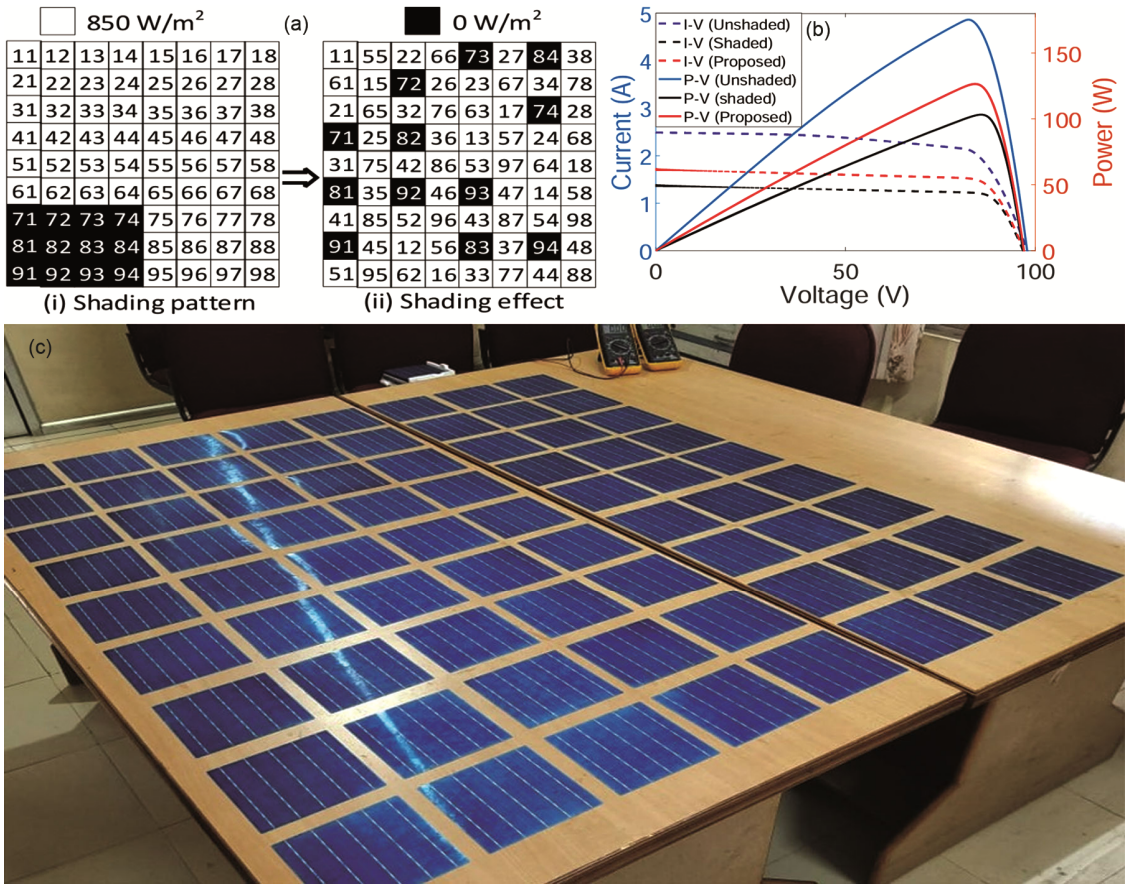

Fig. 8 — 9 ×8 TCT-connected PV array (a) Shading pattern and shading effect, (b) I-V and P-V characteristics of unshaded, shaded and reconfigured array (c) Experimental setup

a reference, the

Table 2 — Simulation results of 9 × 8 TCT-connected PV array

Shading condition	Voltage (V)	Current (A)	Power (W)	Performance degradation
Unshaded	82.4	2.13	175.37	0%
Shaded (Fig. 8(a)(i))	85.85	1.20	103.28	41.12%
Proposed (Fig. 8(a)(ii))	84.3	1.50	126.54	27.84%

Table 3 — Experimental validation of 9 × 8 TCT-connected PV array

Shading condition	Voltage (V)	Current (A)	Power (W)	Performance degradation
Unshaded	79.20	1.82	144.14	0%
Shaded (Fig. 8(a)(i))	77.10	0.96	74.02	48.65%
Proposed (Fig. 8(a)(ii))	78.40	1.41	110.54	23.31%

modules have an irradiance of 850 W/m^2 at a temperature of 27 °C and a global air mass of 1.5 (i.e., AM 1.5g). All the modules are of 3 Wp (at STC) rating, and the datasheet parameters are identical to each other[26]. By using the proposed technique, the reconfigured shading pattern is obtained as shown in Fig. 8 (a) (ii). The current-voltage (I-V) and power voltage (P-V) characteristics obtained for the unshaded, shaded (in normal TCT) and reconfigured (proposed) array are shown in Fig. 8 (b). From the Figure, it is very much clear that the proposed technique shows significantly improved performance compared to the normal TCT-connected array[26]. Simulation results and experimental validation of 9 × 8 TCT-connected is also shown in Table 2 and Table 3, respectively.

4 Conclusion

An algorithm that exhibits a significant performance improvement during PSC is proposed in this work to reduce the performance degradation in TCT-connected PV arrays. According to the simulation results, the proposed algorithm can increase the maximum power of a TCT-connected PV array by more than 35%. The suggested algorithm can be used with TCT-connected PV arrays of various sizes and under various irradiance and temperature conditions.

Acknowledgement

This work was funded by AICTE, Govt. of India under RPS for the NE Region under File No.8-14/FDC/RPS(NER)/POLICY-1/2020-21 dated 10th March 2021.

References

1 Chen Y, Altermatt P P, Chen D, Zhang X, Xu G, Yang Y, Wang Y, Feng Z, Shen H & Verlinden PJ, *IEEE J Photovolt*, 8 (6) (2018) 1531.
2 "Snapshot 2021- executive summary," *IEA-PVPS Newsletter, 2021*.
3 Shongwe S & Hanif M, *IEEE J Photovolt*, 5 (3) (2015) 938.
4 Bonthagorla P K & Mikkili S, *CSEE J Power Energy Syst*, 8 (3) (2020) 682.
5 Babu T S, Ram J P, Dragicˇevic´ T, Miyatake M, Blaabjerg F & Rajasekar N, *IEEE Trans Sustain Energy*, 9 (1) (2017) 74.
6 Changmai P, Nayak S K & Metya S K, *IET Renew Power Gener*, 13 (14) (2019) 2647.
7 Aldaoudeyeh A-M I, *J Engg*, 2018 (5) (2018) 257.
8 Bingo O¨l & Özkaya B, *Sol Energy*, 160 (2018) 336.
9 Jha V, *Iran J Sci Technol Trans A*, 46 (2) (2022) 503.
10 Villa L F L, Picault D, Raison B, Bacha S, and Labonne A, *IEEE J Photovolt*, 2 (2) (2012) 154.
11 Eltamaly A M, Mohamed Y S, El-Sayed A-H M, Mohamed M A & Elghaffar A N A, 5 (1) (2020) 1.
12 Storey J, Wilson P R & Bagnall D, *IEEE Trans Power Electron*, 29 (4) (2013) 1768.
13 Rani B I, Ilango G S & Nagamani C, *IEEE Trans Sustain Energy*, 4 (3) (2013) 594.
14 Potnuru S R, Pattabiraman D, Ganesan S & Chilakapati N, *Renewable Energy*, 78 (2015) 264.
15 Krishna S G & Moger T, *IEEE Trans Energy Convers*, 34 (4) (2019) 1973.
16 Sahu H S, Nayak S K & Mishra S, *IEEE Trans Emerg Sel Topics Power Electron*, 4 (2) (2015) 626.
17 Dhanalakshmi B & Rajasekar N, *Energy Conv Manag*, 156 (2018) 84.
18 Venkateswari R & Rajasekar N, *Energy Conv Manag*, 215 (2020) 112885.
19 Storey J P, Wilson P R & Bagnall D, *IEEE Trans Power Electron*, 28 (6) (2012) 2946.
20 Da Rocha M V, Sampaio L P & da Silva S A O, *Sustain Energy Technol Assess*, 40 (2020) 100761.
21 Qi J, Huang X, Ye B & Zhou D, *CSEE J Power Energy Syst*, 9 (2) (2022) 733.
22 Ye B, Qi J, Li Y, Xie L & Yang F, *IEEE Conference on Energy Internet and Energy System Integration (EI2)*, IEEE, (2017) 1.
23 Bastidas-Rodr´ıguez J D, Cruz-Duarte J M & Correa R, *IEEE J Photovolt*, 9 (3) (2019) 768.
24 Pillai D S, Ram J P, Nihanth M S S & Rajasekar N, *Energy Conv Manag*, 172 (2018) 402.
25 Mahmoud Y & El-Saadany E F, *IEEE J Photovolt*, 7 (6) (2017) 1746.
26 "https://www.enfsolar.com/PV/panel- datasheet/crystalline/," *WAAREE, India*.